Porous Hollow Carbon Nanospheres Embedded with Well-Dispersed Cobalt Monoxide Nanocrystals as Effective Polysulfide Reservoirs for High-Rate and Long-Cycle Lithium-Sulfur Batteries

Shikui Wu,[*#a] Yingze Wang,[#b] Shengsang Na,[*c] Chaojun Chen,[a] Tengfei Yu,[a] Huanyun Wang,[a] and Huimin Zang,[a]

[a] College of Pharmacy, Inner Mongolia Medical University, No.5 Xinhua west street, Hohhot 010059, PR China. *E-mail: shikuiwu@yahoo.com, Fax:+86 04716653172, Tel: +86 04716653172.

[b]. College of biological science and engineering, Hebei university of science and technology, No.26 Yuxiang street, Shijiazhuang, Hebei, P.R. China 050018

[c] Academy of Mongolia Medicine, Inner Mongolia Medical University, No.5 Xinhua west street, Hohhot 010059, PR China.

#Dual contributors

Table S1. Performance comparison of CoO/HCN material with other representative host materials in literatures [13,19,33,47,48,50–56].

Ref.	Host material (morphology)	Current rate (C)	Cycle number	Capacity (mAh g^{-1})	Capacity retention (%)
This work	CoO nanocrystals embedded HCN	0.2	200	996	80.2
		1.0	1000	629	66.9
		2.0	1000	482	57.4
[17]	Polypyrrole-MnO_2 Coaxial Nanotubes	1.0	500	550	65.0
[23]	cobalt and N-doped graphitic carbon	1.0	500	625	54.3
[37]	TiO_2 coated N-doped graphene	1.0	500	628	57.0
[51]	Nitrogen-doped double-shelled hollow carbon spheres	0.5	200	520	62.0
[52]	Nitrogen-doped hollow carbon nanospheres	0.2	100	980	88.0
[54]	PANI shell	0.2	200	780	67.8
[55]	PEDOT coated rGO/ZIF-8	0.2	100	927	70.8
[56]	TiO_2 hollow spheres	0.5	700	580	53.1
[57]	Hydrogen reduced TiO_2	0.2	200	890	80.9
[58]	TiN nanotube	0.5	500	644	65.2
[59]	$Si/SiO_2@C$	0.2	100	833	78.2

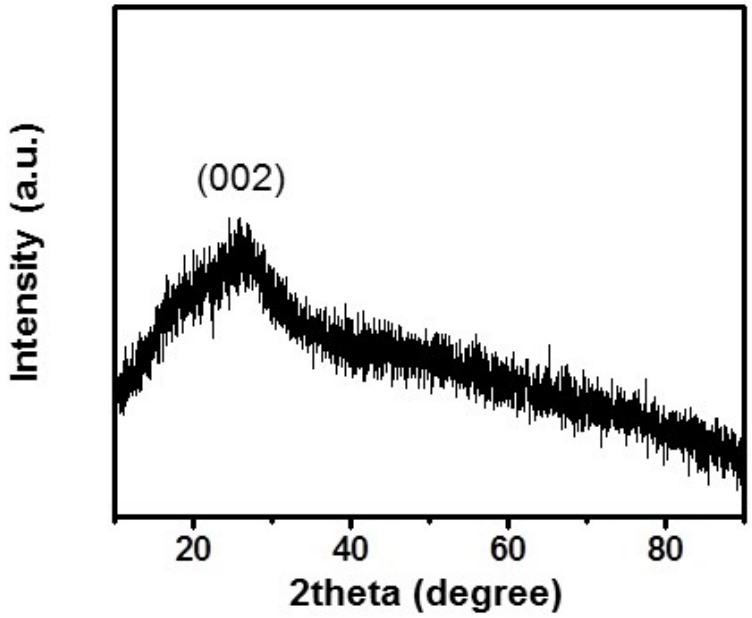

Fig. S1. XRD pattern of the HCN material, showing the typical diffraction peak of carbonaceous material.

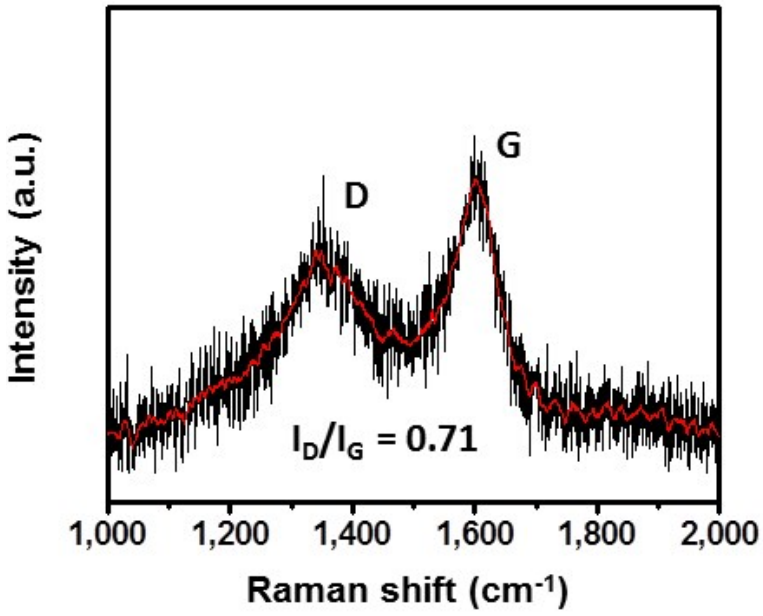

Fig. S2. Raman spectrum of the HCN material. The intensity ratio of D and G band is *ca*. 0.71, suggesting the moderate graphitic degree of carbon.

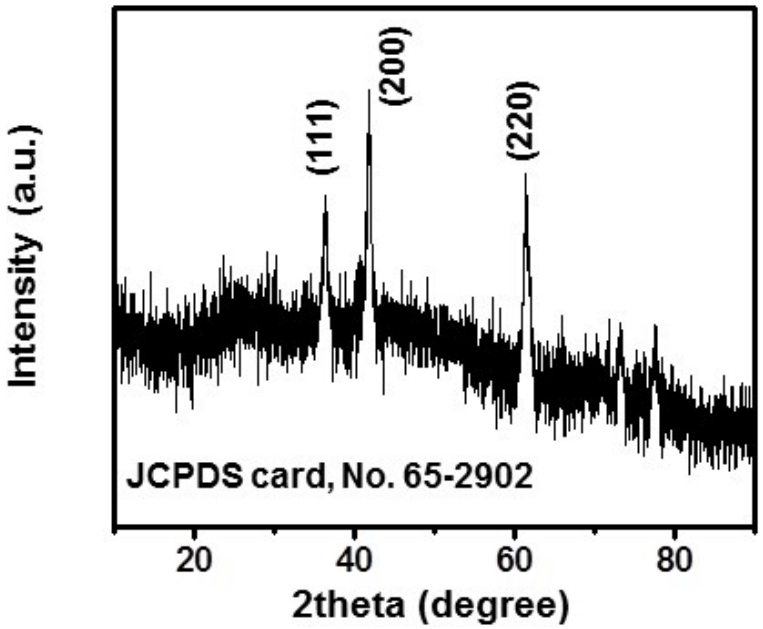

Fig. S3. XRD pattern of the CoO/HCN material. The observed diffraction peaks can be ascribed to the CoO (JCPDS card, No. 65-2902).

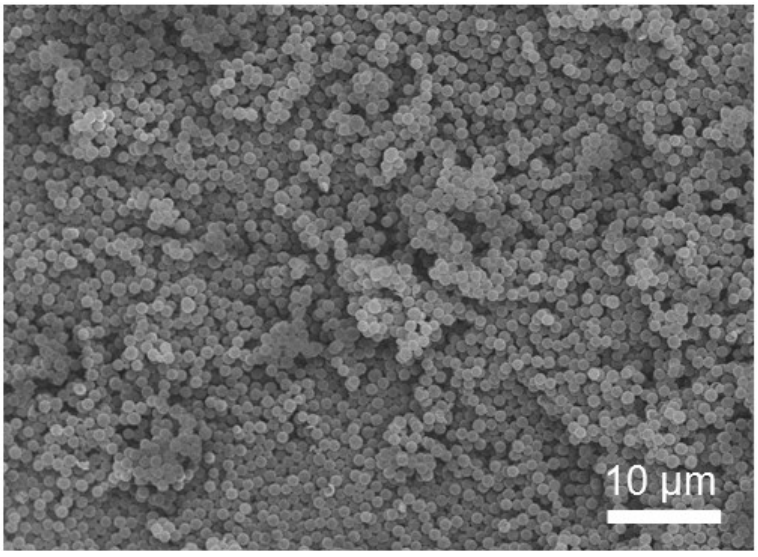

Fig. S4. SEM image of the SiO_2@RF material. The SEM observation reveals the uniform distribution of SiO_2@RF nanospheres.

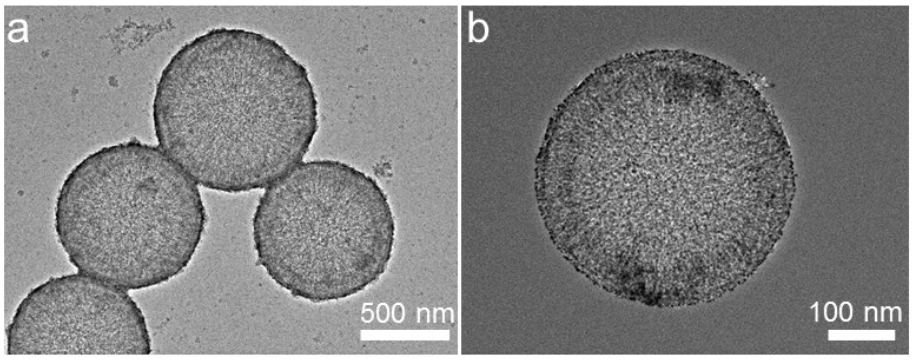

Fig. S5. TEM images of CoO/HCN-S composite, showing the morphology similar to that of CoO/HCN material.

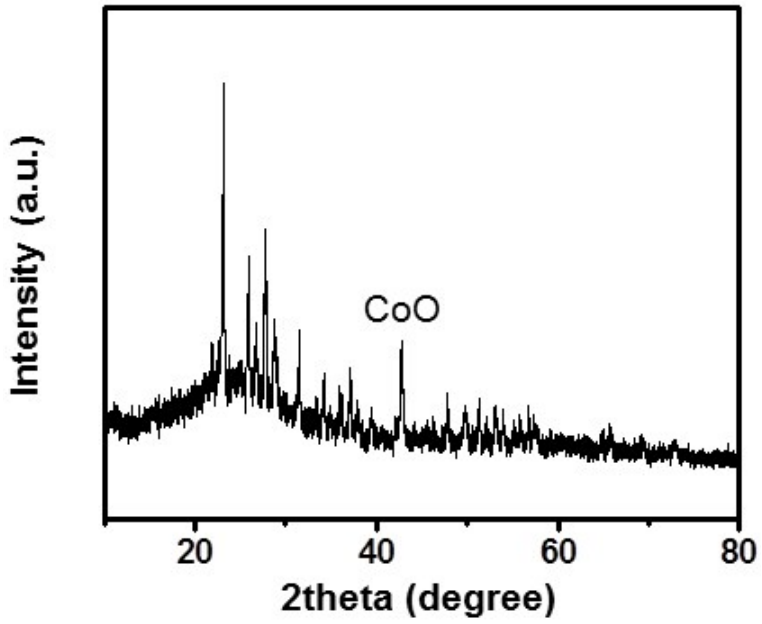

Fig. S6. XRD pattern of the CoO/HCN-S composite. The observed diffraction peaks can be ascribed to HCN material, CoO nanocrystals and sulfur powder.

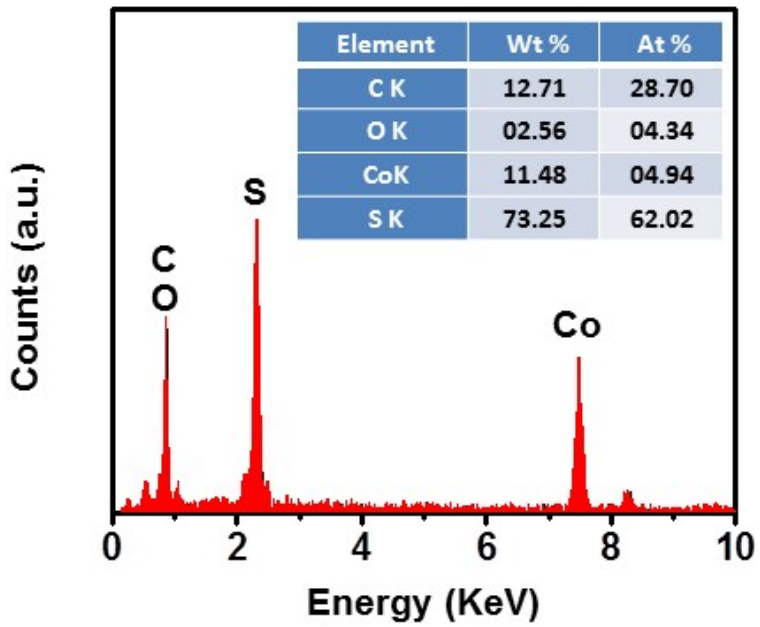

Fig. S7. EDX spectrum of the CoO/HCN-S composite. The EDX spectrum suggests the co-existence of C, Co, O and S elements, and the sulfur content was measured to be 73.3 wt.%.

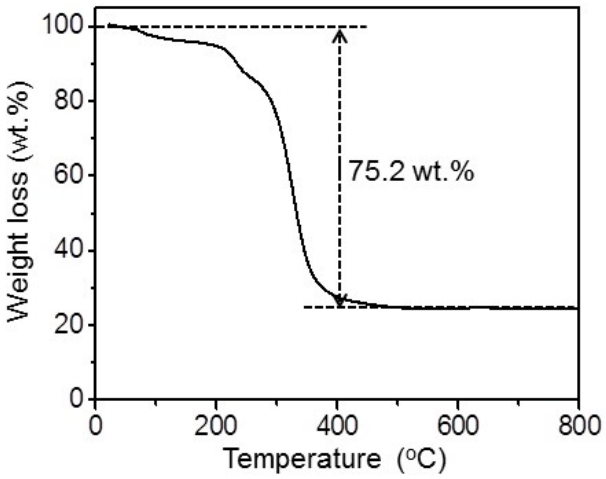

Fig. S8. TGA curve of CoO/HCN material annealed under air from room temperature to 800 °C.

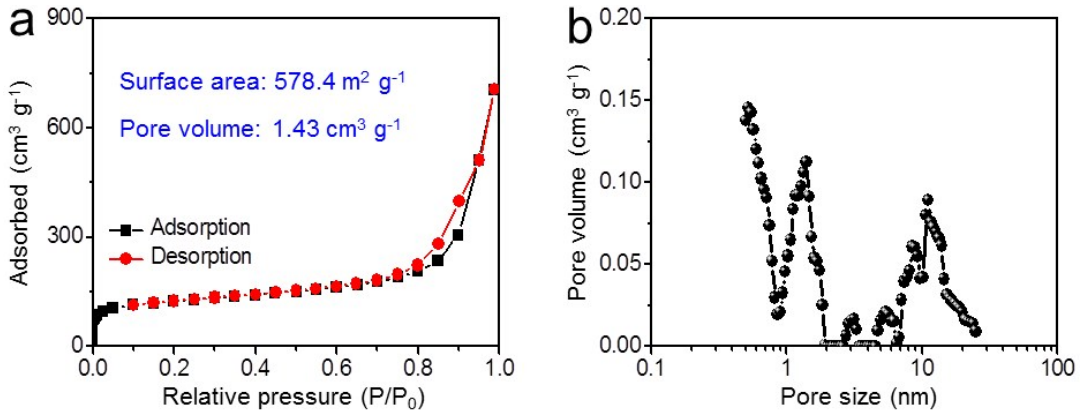

Fig. S9. (a) N_2 adsorption/desorption isotherms and (b) pore size distribution of CoO/HCN material.

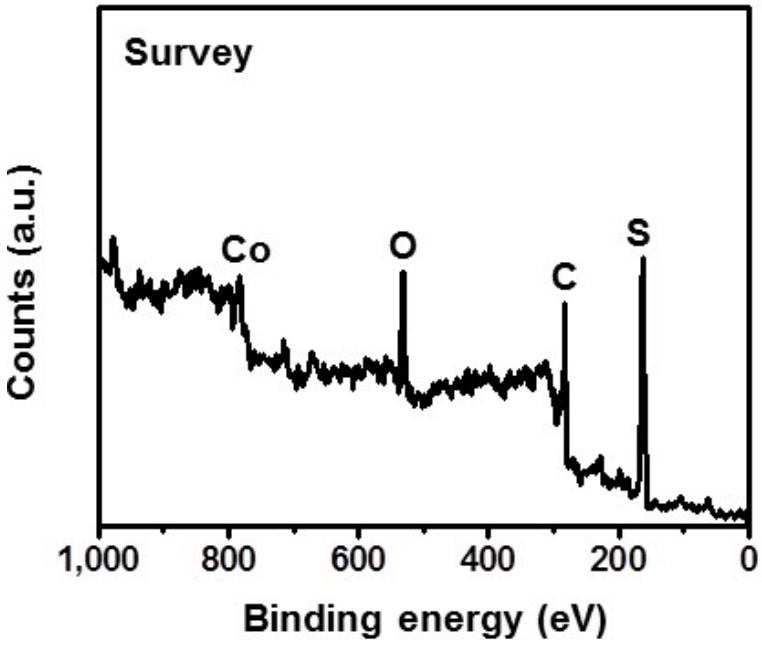

Fig. S10. Survey XPS spectrum of the CoO/HCN-S composite. C, Co, O and S elements are detected, consistent with the result of EDX spectrum.

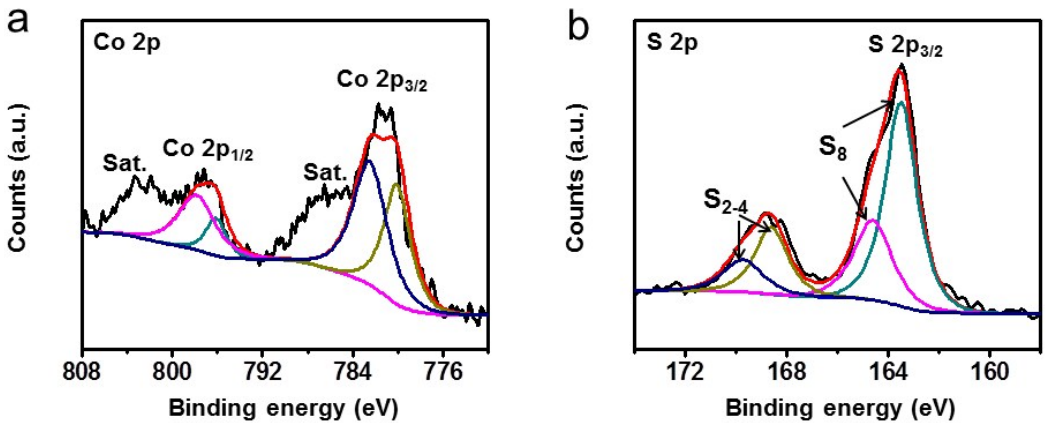

Fig. S11. XPS results of CoO/HCN-S composite. High-resolution XPS spectrum at (a) Co 2p region and (b) S 2p region.

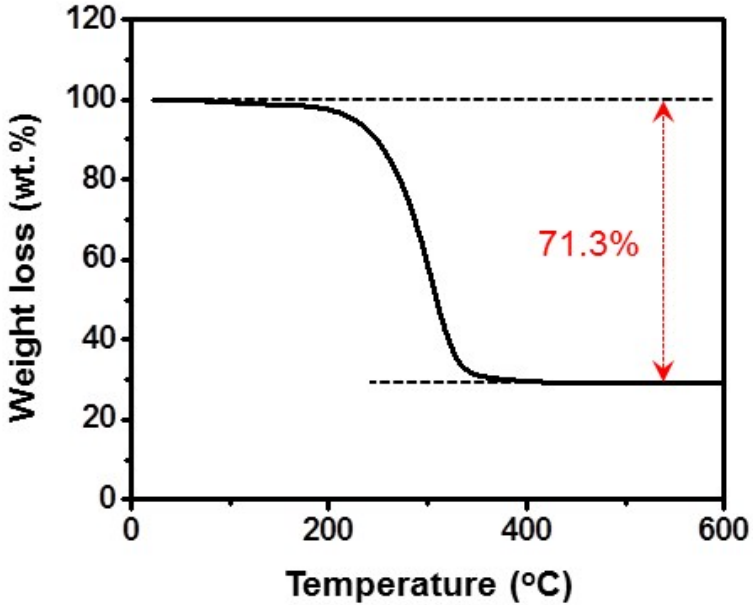

Fig. S12. Thermo gravimetric analysis (TGA) curve of CoO/HCN-S composite under N_2 atmosphere from room temperature to 600 °C with ramping rate of 10 °C/min. The sulfur content is determined to be 71.3 wt.%.

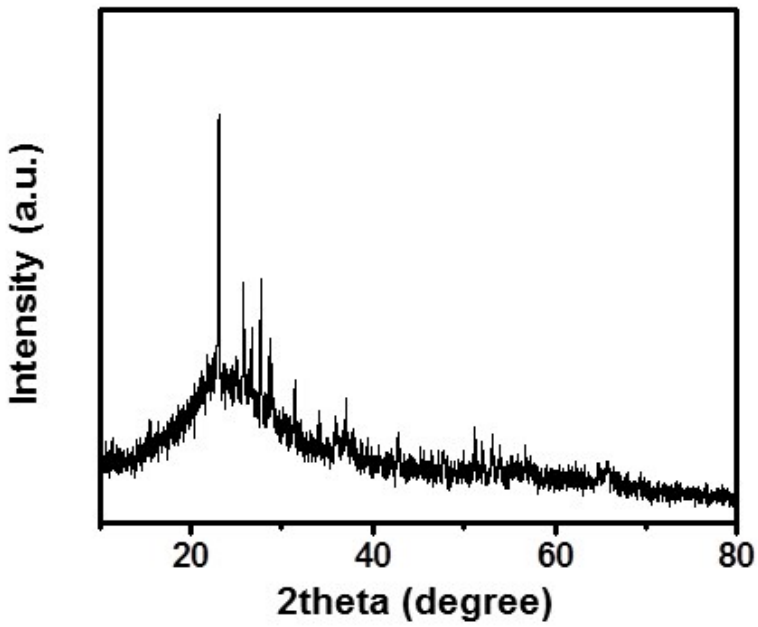

Fig. S13. XRD pattern of the HCN-S composite, indicating the existence of sulfur in HCN-S composite.

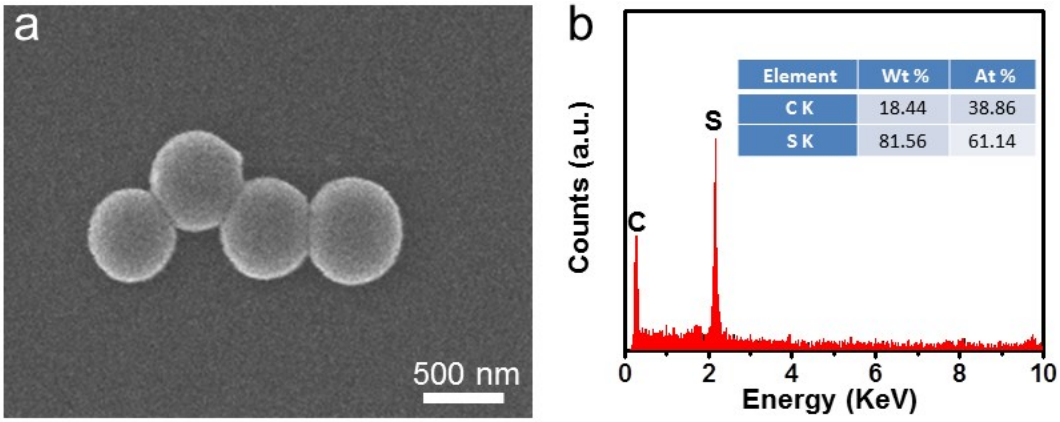

Fig. S14. Morphology and composition characterizations of HCN-S composite. (a) SEM image and (b) EDX spectrum of HCN-S composite.

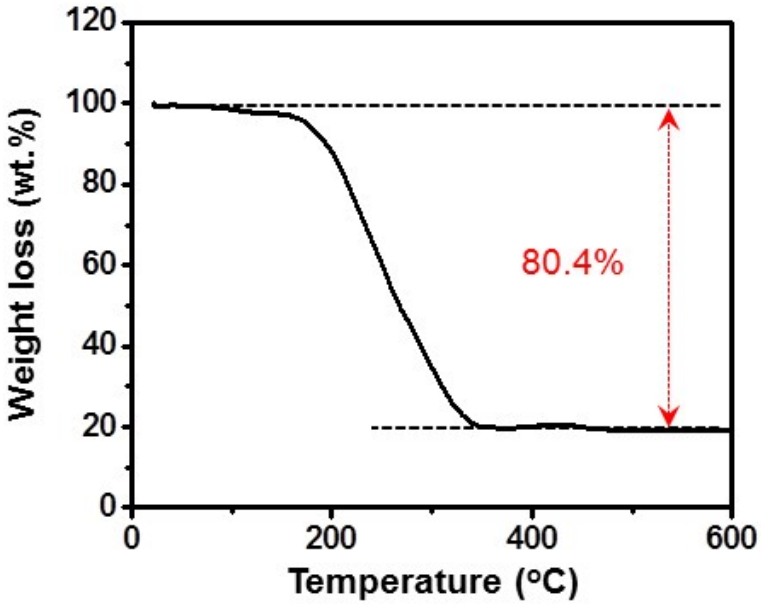

Fig. S15. TGA curve of HCN-S composite under N_2 atmosphere from room temperature to 600 °C with ramping rate of 10 °C min^{-1}. The sulfur content is determined to be 80.4 wt.%.

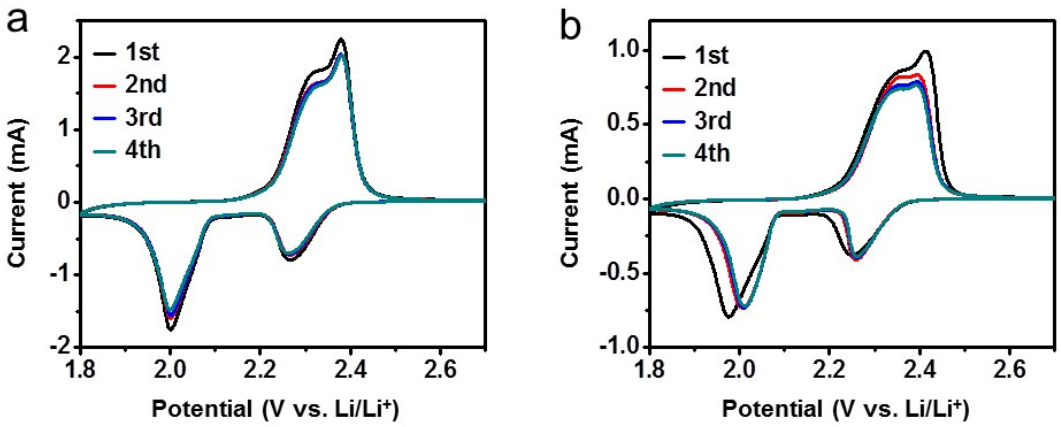

Fig. S16. CV curves of (a) CoO/HCN-S and (b) HCN-S composite cathodes at a scan rate of 0.2 mV s^{-1}.

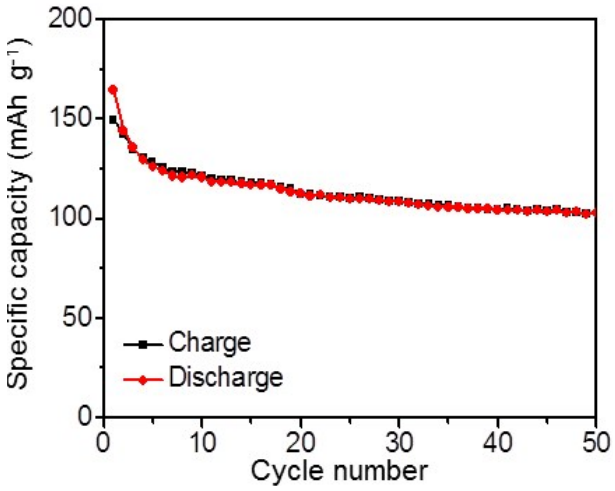

Fig. S17. Electrochemical performance of CoO/HCN material as anode in lithium-ion batteries at 100 mA g^{-1}.

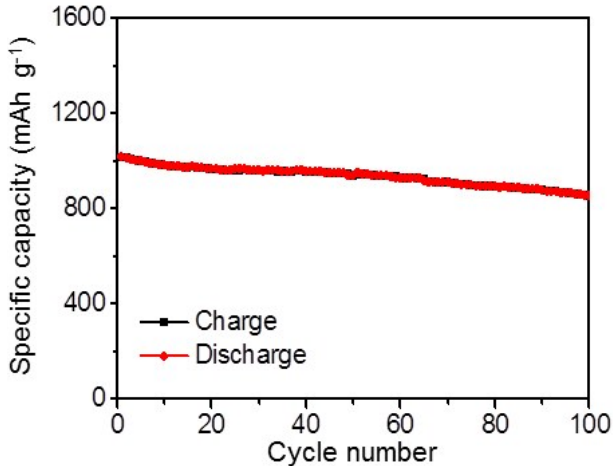

Fig. S18. Cycling performance of CoO/HCN-S composite cathode at 1.0 C in the electrolyte without $LiNO_3$ additive.

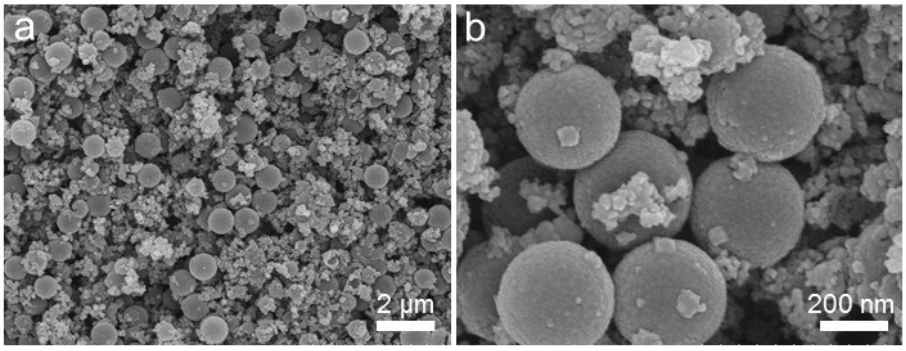

Fig. S19. (a,b) Morphology characterization of CoO/HCN-S composite after cycling for 1000 cycles at 2.0 C. The SEM observations reveal the structure similar to that of CoO/HCN material, indicating its highly structural integrity.